REGULAR PAPER

**Hua Zhang · Muhammad Yamin Younis ·
Bo Hu · Hong Wang · Xuee Wang**

Investigation of attachment saddle point structure of 3-D steady separation in laminar juncture flow using PIV

Abstract An experimental study of laminar horseshoe vortex upstream of a cylinder/flat plate juncture has been conducted using PIV in symmetric plane to verify the existence of attachment saddle point topology. The experimental results confirm the existence of attachment saddle point structure, which is different from conventional separation saddle point flow topology. In one, two and three primary vortices condition, upstream streamlines near surface do not rise up or separate from the plate surface but attach to plate surface. The outmost vortex initiates from the spatial singular point and not from surface singular point. Especially, the skin-friction-lines convergence corresponds to spatial attached flow but not separated flow as in case of conventional separation saddle point topology, alternatively, the spatial attached flow correspond to convergent but not divergent skin-friction-lines, as happens in conventional attachment flows. The results indicate that attachment saddle point structure is a kind of separation in which vorticity separates from spatial layer of boundary layer but not from the plate surface. The study also reveals three types of attachment saddle point topologies, these three topologies all satisfy the topological, singular point index rule.

Keywords Juncture flow · 3-D steady separation · Attachment saddle point · PIV

1 Introduction

The conventional point of view about three-dimensional boundary layer separation implies, the spatial vortex is separated from the surface boundary layer under certain adverse pressure gradient, the spatial vortex sheet issued from the convergent skin-friction-line, or in other words, as skin-friction-lines converge the near-surface streamlines may rise up or separate from the surface and forms the spatial vortex. Maskell (1955), Lighthill (1963) and Wang (1972, 1976) used different separation modes to describe steady three-dimensional boundary layer separation, though the three descriptions are slightly different from each other, they all represent the conventional mechanism of steady three-dimensional boundary layer separation: as skin-friction-lines converging, the limiting streamlines may rise up from the surface and forms the spatial vortex. Lighthill (1963) described the skin-friction-line convergent asymptote that issued from surface saddle point as three-dimensional separation line. Figure 1 shows the conventional topology (Baker 1979) of horseshoe vortex in symmetry plane upstream of juncture and associated skin-friction-line extracted using oil-flow visualization. The oil-flow visualization experiment is performed in wind tunnel at Beihang University. In the symmetric plane view of Fig. 1, the outmost vortex sheet is separated from the plate surface.

H. Zhang (✉) · M. Y. Younis · B. Hu · H. Wang · X. Wang
Ministry of Education Key Laboratory of Fluid Mechanics, School of Aeronautical Science and Engineering,
Beihang University (BUAA), Beijing 100191, People's Republic of China
E-mail: ltszhh@buaa.edu.cn
Tel.: +86-130-11033580
Fax: +86-10-82313570
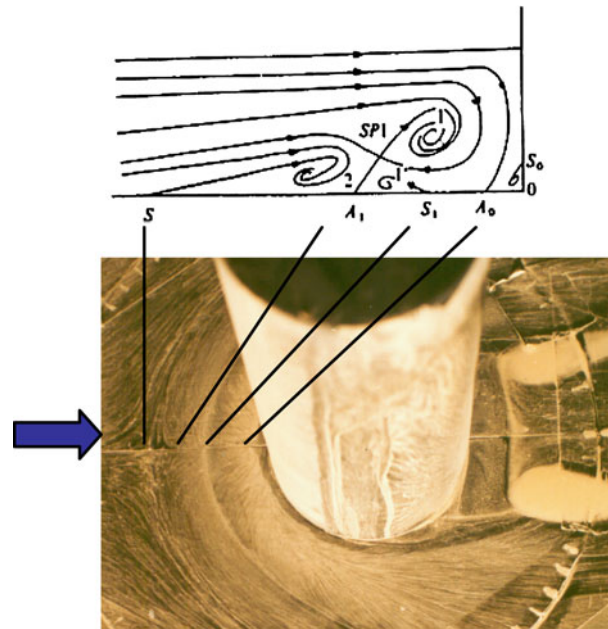
Fig. 1 The conventional separation topology (Baker 1979) and surface oil-flow visualization ($Re_D = 1.36 \times 10^5$)

The juncture flow structure about outmost singular point is schemed in Fig. 2. In the symmetry plane, the flow topology is a separation half saddle point structure, whereas in the spatial separation surface or vortex sheet, the flow topology is a separation half node point structure. On the plate surface, the convergent asymptote of skin-friction-line originating from the saddle point is always taken as three-dimensional separation line, which is also the place of emergence of spatial vortex sheet. The saddle point on plate surface is called separation saddle point (S_s) and this conventional 3-D separation structure is called separation saddle point structure. This conventional 3-D steady separation topology has been well accepted and is widely applicable in analysis of 3-D steady separation flows.

However, Visbal (1991) through his numerical simulation of laminar horseshoe vortex structure for circular cylinder/flat plate juncture revealed a different vortex topology in symmetry plane of the juncture as shown in Fig. 3, in which streamlines near surface do not rise up or separate from the plate surface but attaches to it. In symmetry plane upstream of the juncture, the singular point is a half node as shown in Fig. 3a, c, this is the typical feature of attachment saddle point structure in which the outmost saddle point on plate surface is not a separation saddle point but an attachment saddle point (detailed description of attachment saddle point structure will be presented in Sect. 3 with reference to Fig. 14a). The numerical simulation of juncture flow of Hung et al. (1992), Chen and Hung (1992), Puhak et al. (1995), Rizetta (1994), and Chen (1995) also revealed attachment saddle point topologies similar to Visbal's result. An experimental study on attachment saddle point structure was contacted by Coon and Tobak (1995), they used laser light sheet and long-time exposure tracing visualization method to study the cylinder/plate juncture and shown the attachment saddle point structure according to their visualization result of Fig. 3b. But the qualitative method of laser light sheet and long-time exposure tracing visualization of Fig. 3b still lacks sufficient spatial resolution to identify the details of attachment saddle point topology. Seal et al. (1995) used PIV to show the topology of juncture's unsteady laminar horseshoe vortices, they found the topology in downstream breakaway regime was "essentially identical to steady attachment topology described by Visbal (1991)". According to Visbal's (1991) results, attachment in downstream region corresponds to conventional divergent-limiting streamlines, none but outmost attachment singular point corresponds to convergent-limiting streamlines. Whereas in Seal et al's (1995) downstream breakaway regime, the corresponding convergent-limiting streamline is not confirm. Seal et al. (1997) affirmed the attachment structure (spatial attachment and convergent on surface) occurs in outmost singular point position (as shown in their Fig. 2), but they did not give details of the attachment structure. As a matter of fact, this unconventional topology of separation flow is far from those were widely accepted. Yet our understanding about attachment saddle point structure is still limited. The purpose of the present study is to experimentally verify the attachment saddle point structure in 3-D steady laminar juncture flow using quantitative method of PIV, and to study the possible topologies of attachment saddle point structure.

Fig. 2 Conventional separation saddle point structure
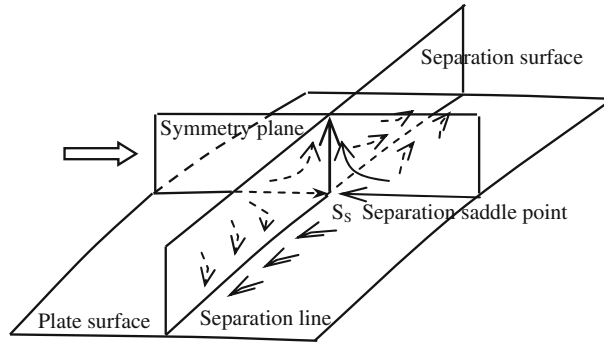
(a) Numerical simulation **(b)** Laser light sheet visualization **(c)** Topology
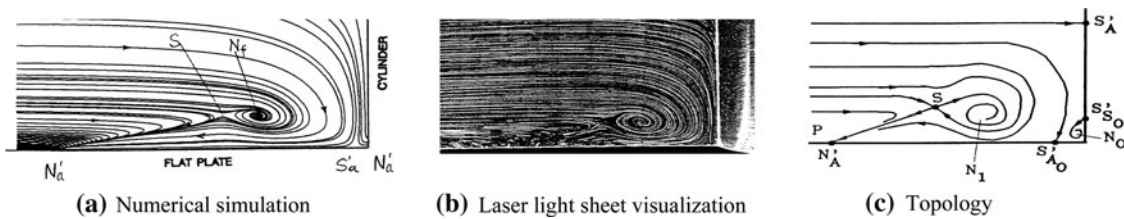
Fig. 3 Visbal's (1991) numerical simulation (**a**), Coon and Tobak's (1995) laser light sheet visualization result (**b**) and the corresponding topology (**c**) of attachment saddle point structure

2 Experimental apparatus and techniques

The experiments were conducted in a low-speed water channel at Fluid Mechanics Institute of School of Aeronautical Science and Engineering of Beihang University, with test section size of 400×400 mm^2 and length of 4 m. A flat plate with 5/1 elliptic leading edge and length of 600 mm was installed in the water channel and three circular cylinder models with diameter $D = 50$, 65 and 80 mm with height $H = 200$ mm were mounted on the flat plate to form the junctions. The end of cylinders were submerged in the water at least 5 cm below the free surface of the water and the aspect ratio of cylinders H/D were larger than 2.0 so that to prevent the influence of the end. The experimental free-stream velocity was fixed at about 3 cm/s, so that the experimental Reynolds number defined by cylinder diameter ranges from Re$_D = 1,000$–3,000, within this range of Reynolds number, the juncture flow exhibits steady laminar three-dimensional horse-shoe vortex characteristics.

The experiments were carried out using a 2-D PIV system which consists of dual-cavity pulse Nd:Yag laser with $\Delta t = 200$–600 ns and power of 200 mJ/pulse, laser sheet arm, laser pulse synchronizer and CCD camera with spatial resolution of $1,600 \times 1,200$ pixels and with data sampling frequency 30 frames/s. The particles were hollow glass particles with diameter of 5–10 μm and the specific gravity is about 1.05. The PIV experiment setup is shown in Fig. 4. The experiment model configuration is shown in Fig. 5.

Before the circular cylinders were mounted on the flat plate, the incoming steady laminar boundary layers were tested using PIV to verify the velocity profiles, at the point where the centre of the cylinders were placed and in velocity range of 3–9 cm/s. Comparisons of the experimental boundary layer velocities profiles for various free-stream velocities with that of Blasius are shown in Fig. 6 and found in good agreement. Comparison of experimental velocity data and that of Blasius are shown in Table 1. In the present study, the boundary layer condition of first row of Table 1 is used.

3 Experimental results and discussion

Figure 7 shows attachment structure's velocity vector distribution and streamline patterns of symmetry plane upstream of cylinder/plate juncture at Reynolds number Re$_D = 1,600$, 2,000 and 2,400. The results indicate that the flow structures were steady in this Reynolds number range. A more detailed instantaneous streamline structures are shown in Figs. 8 and 9. It is observed that whether for one primary vortex case at
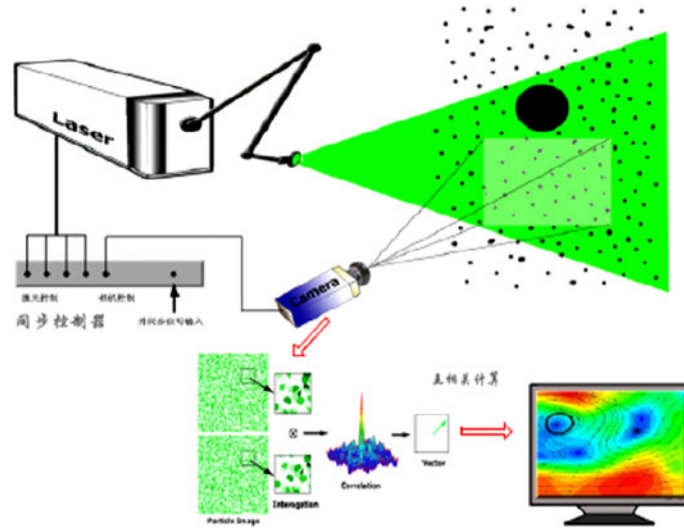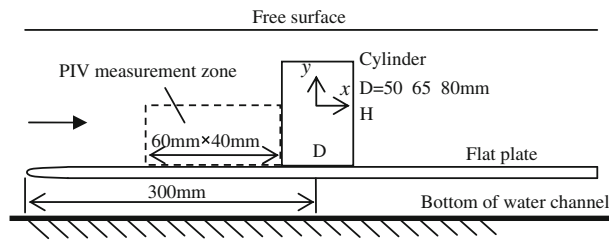
Fig. 4 PIV experiment setup

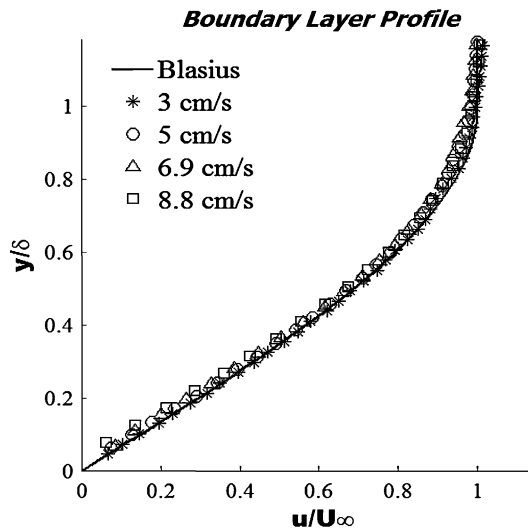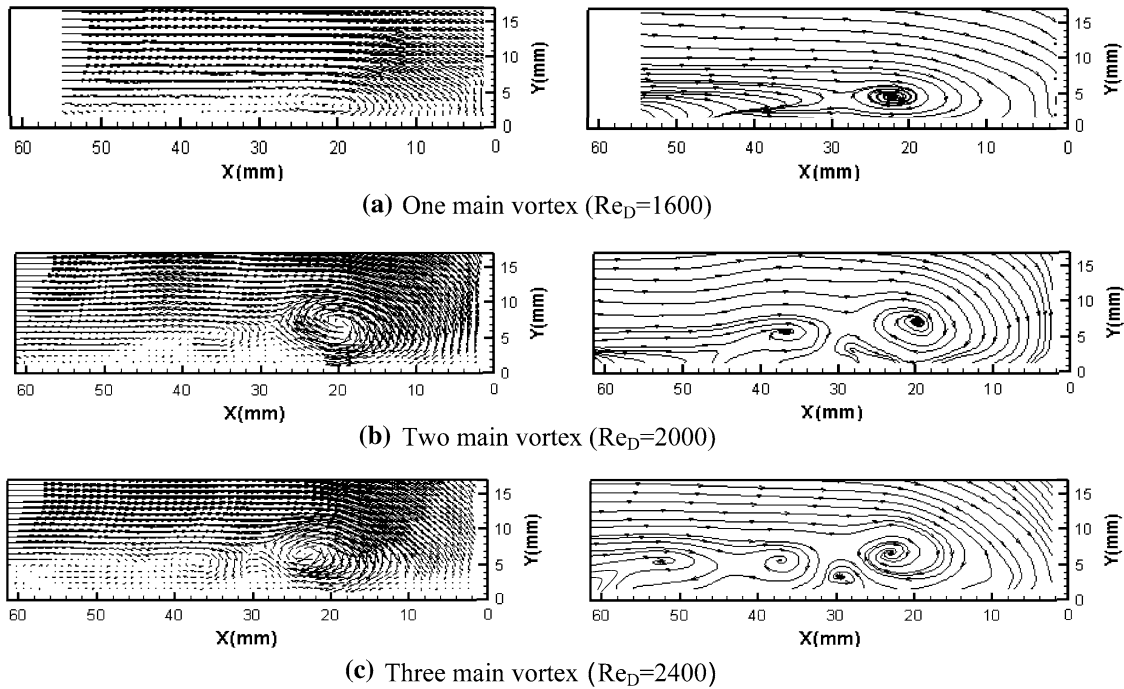**Fig. 5** Experimental model configuration and PIV measurement zone

Fig. 6 Comparison of PIV-tested velocity profiles and Blasius profile in experimental free-stream velocity range

$Re_D = 1,600$ or two and three primary vortices at $Re_D = 2,000$ and 2,400, the upstream streamlines near plate surface do not rise up or separate from the plate surface but attach to the plate surface, a characteristic feature of attachment saddle point topology. The flow topologies inferred from the above experimental results are indicated in Fig. 10 as they were first given by Visbal (1991), and the comparison to conventional separation vortex topologies is shown in Fig. 11. The distinctive difference between two types of topologies

Table 1 Comparison of experimental and Blasius B.L data

U_∞ (mm/s)	Re_x	Blasius δ (mm)	Exp. $u = 0.99\,U_\infty$ (m/s)	Exp. δ (mm)	Errors of δ
30	8,957	15.8	29.8	16	0.013
50	14,928	12.3	49.6	12.4	0.008
69	20,600	10.4	68.4	10.6	0.019
88	26,273	9.25	87.1	9.7	0.048

(a) One main vortex (Re_D=1600)

(b) Two main vortex (Re_D=2000)

(c) Three main vortex (Re_D=2400)

Fig. 7 Attachment structure's velocity vectors (*left*) and streamlines (*right*) in symmetry plane of cylinder/plate juncture measured by PIV

in symmetry plane are following two points: firstly, for conventional separation topology, the outmost singular point is a half separation saddle point (Fig. 11), but for attachment topology, the outmost singular point is an attachment half node (Fig. 10); secondly, for conventional separation topology, the outmost vortex (focus) issued from the surface half saddle point (Fig. 11), but for attachment topology, the outmost vortex issued from a spatial saddle point (Fig. 10). Although the spatial topologies of two vortex structures in symmetry plane are completely different from each other, both spatial topologies correspond to a similar skin-friction-line structure as compared using numerical simulation in Figs. 12 and 13, which are taken from Wang et al. (2010). Since the experimented Reynolds number was rather small to get skin-friction-line pattern on plate surface using oil-flow visualization, so the numerical simulation was utilized to verify the relationship of spatial topologies and limit-streamline structures on plate surface. It is well acknowledged that the limiting-streamlines near plate surface have identical topological features with skin-friction-line. The detailed flow structure about outmost singular point inferred from the above analysis can be schemed in Fig. 14a, and the conventional attachment flow structure is shown in Fig. 14b for comparison. It is shown by comparing the flow structure of Fig. 14a with that of conventional separation saddle point structure of Fig. 2 that, although both spatial flow structures (separation and attachment) are completely different from each other, the skin-friction-lines on plate surface always converge to an asymptote issued from a saddle point on the plate surface. It is also shown by comparing flow structure of Fig. 14a with conventional attachment structure of Fig. 14b, although both spatial flow structures are similar (i.e., both are attachment flow), their skin-friction-line structures are completely different (i.e., one is a convergent asymptote whereas another is a divergent asymptote).

Because the outmost saddle point on plate surface shown in Fig. 14a corresponds to a spatial attachment flow rather than a spatial separation flow, so that the flow structure in Fig. 14a is called attachment saddle
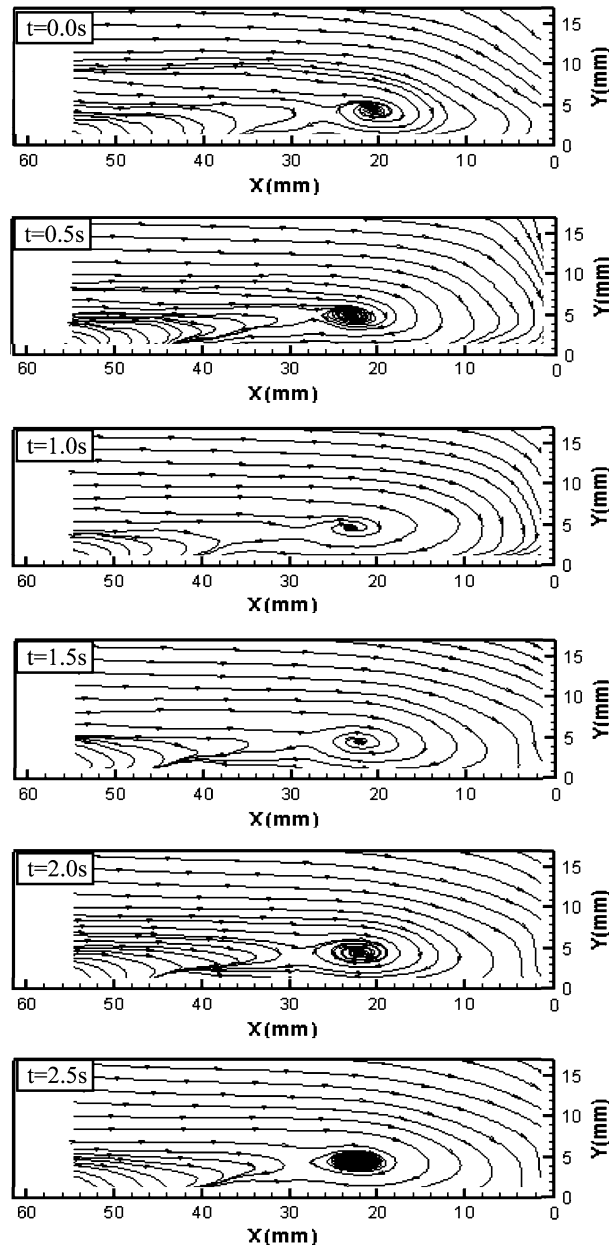
Fig. 8 Time series of streamline of one main vortex structure given by PIV (Re$_D$ = 1,600)
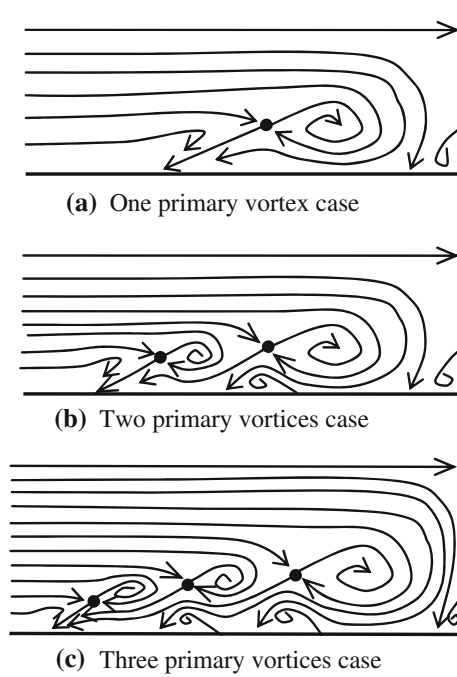
point structure of juncture flow. This name "Attachment Saddle Point" not only reflects the feature of half attachment node in symmetric plan but also is a combine representation of half node in symmetric plan, half saddle in attachment surface and a full saddle on plate surface. The flow structures of Figs. 7, 8, 9, 10, 13 (with half attachment node in symmetric plane, similar to symmetric plane of attachment topology in Fig. 14a), represent attachment saddle point structure. Especially, attachment saddle topology is characterized that skin-friction-lines convergence correspond to spatial attached flow but not separated flow as in case of conventional separation saddle point topology, in other words, the spatial attached flow corresponds to convergent but not divergent skin-friction-lines as happens in conventional attachment flows. This again confirms the important deduction given by Visbal (1991) that skin-friction-line convergence is only necessary but not sufficient condition of 3-D steady separation. Perry and Fairlie (1974) indicated the possible existence of attachment saddle point topology in their analysis, yet they did not question the important implications for the interpretation of oil-flow visualizations. Zhang (2005) in his analysis presented the mathematical conditions for flow separation and attachment, and indicated that convergent or divergent
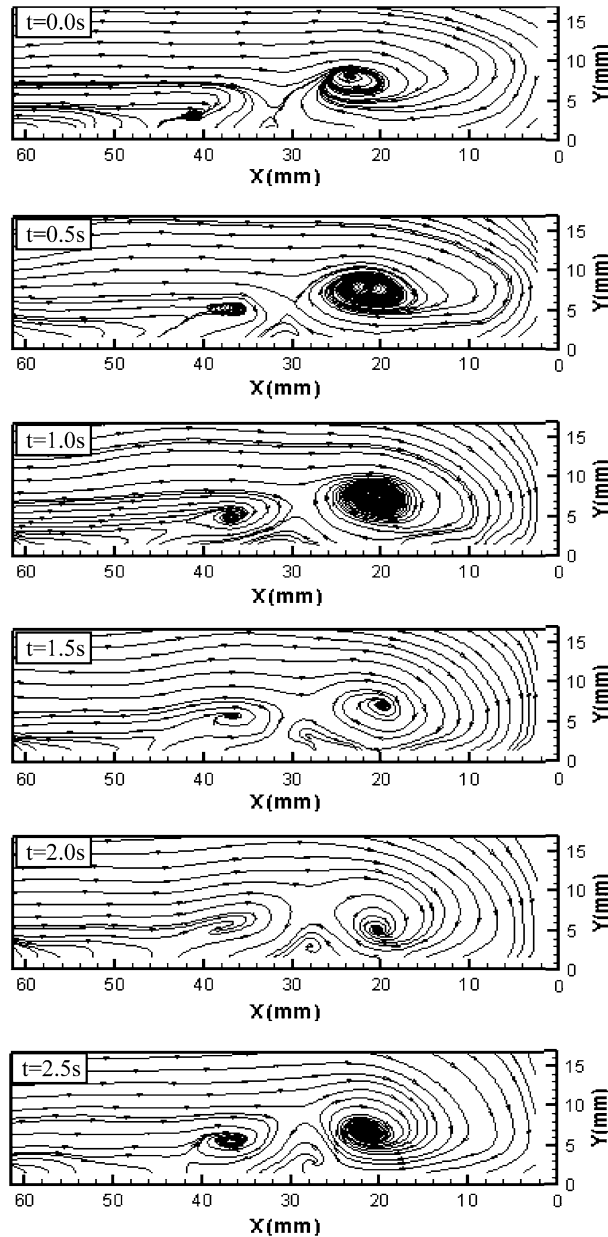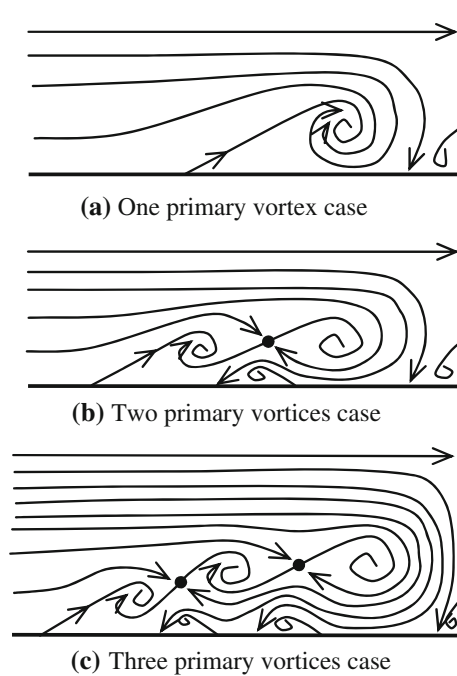
Fig. 9 Time series of streamline of two main vortex structures given by PIV ($Re_D = 2,000$)

asymptote of skin-friction-line may also be attachment line, and he called the convergent asymptote of skin-friction-line as the secondary type of attachment line. This kind of convergent attachment line is rarely seen in reality but the special vortex structure gained in juncture flow is one of the examples. The convergent asymptote of limiting streamline in Figs. 13b and 14b is so called secondary attachment line.

For attachment saddle point structure of juncture flow, the outmost vortex issued not from the plate surface but from a spatial saddle point, this fact brought important question as follows: where does the spatial vortex vorticity come from? Where does upstream vorticity near boundary layer bottom go? From the PIV experiment result, we noticed that horseshoe vortex system was limited in the height of boundary layer as shown in Fig. 15a, b, which is unlike the conventional 3-D separation where vortices depart from the surface. In Fig. 15b, the streamline passing through the spatial saddle point S partitions the incoming boundary layer into up-layer and lower-layer. The vorticity of spatial vortex comes from the up-layer of the boundary layer where enough vorticity exists. In other words, the vortex does not separate from the boundary layer bottom but from a spatial layer which started from spatial saddle point S as shown in

(a) One primary vortex case

(b) Two primary vortices case

(c) Three primary vortices case

Fig. 10 Attachment topologies (Visbal 1991) in symmetry plane of juncture

(a) One primary vortex case

(b) Two primary vortices case

(c) Three primary vortices case

Fig. 11 Conventional topologies (jet maze mode, Baker 1979) in symmetry plane of juncture

Fig. 15b, and the vortex vorticity will be transported to downstream along with two legs of horseshoe vortex. Whereas the upstream vorticity in lower-layer does not pile up in front of singular point but be transported to downstream along with 3-D flow around two sides of the juncture.

The common features of conventional separation topologies indicate that outmost singular point on plate surface is a separation saddle point and outmost spatial vortex originates from plate surface. In addition, downstream vortex topologies may present some difference. Three typical conventional separation
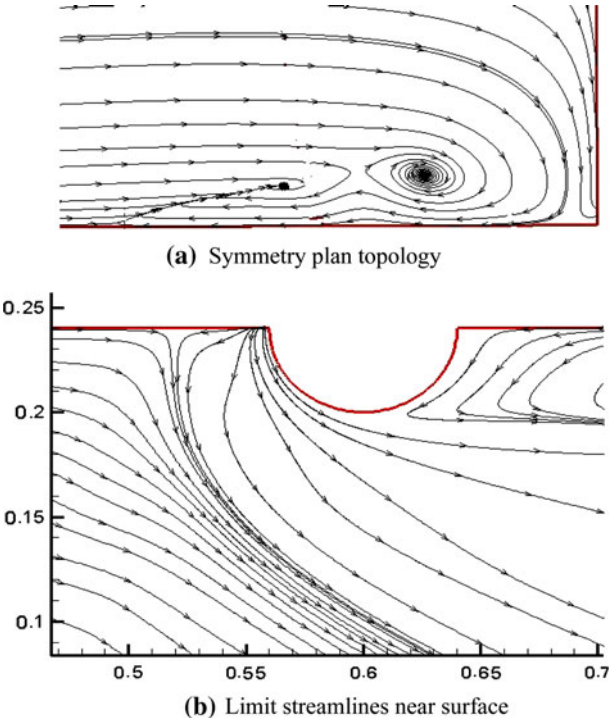
(a) Symmetry plan topology

(b) Limit streamlines near surface

Fig. 12 Simulation result of conventional topologies of circular cylinder/flat plate juncture, $Re_D = 1,000$ (Wang et al. 2010)

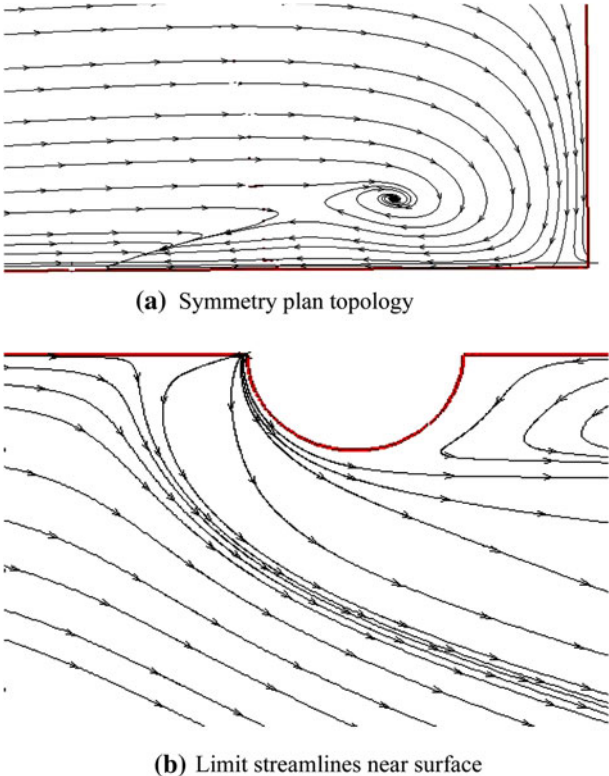
(a) Symmetry plan topology

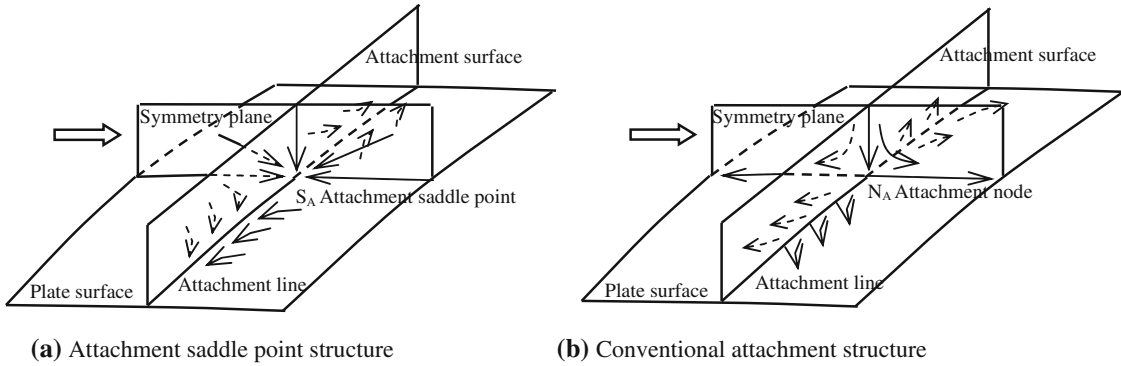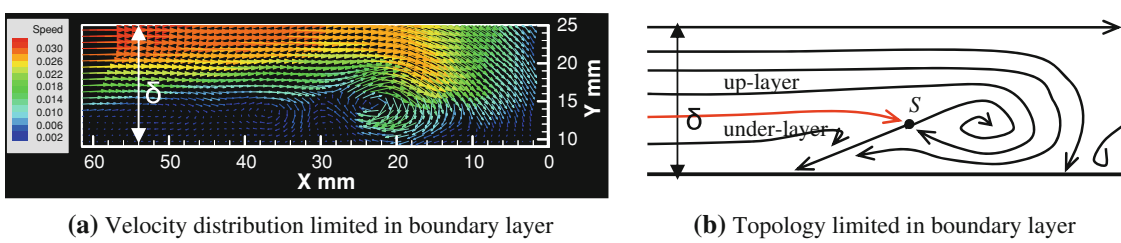(b) Limit streamlines near surface

Fig. 13 Simulation result of attachment topologies of circular cylinder/flat plate juncture, $Re_D = 500$ (Wang et al. 2010)

(a) Attachment saddle point structure   (b) Conventional attachment structure

Fig. 14 Comparison of new attachment saddle point structure and conventional attachment structure

(a) Velocity distribution limited in boundary layer   (b) Topology limited in boundary layer

Fig. 15 Attachment saddle point topology was limited in boundary layer

(a) Stair-step mode   (b) Jet maze mode   (c) Alternative mode
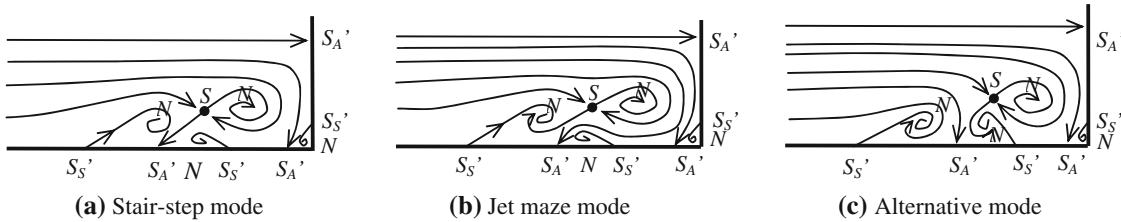
Fig. 16 Three conventional separation saddle point topologies

(a) Attachment topology A   (b) Attachment topology B   (c) Attachment topology C
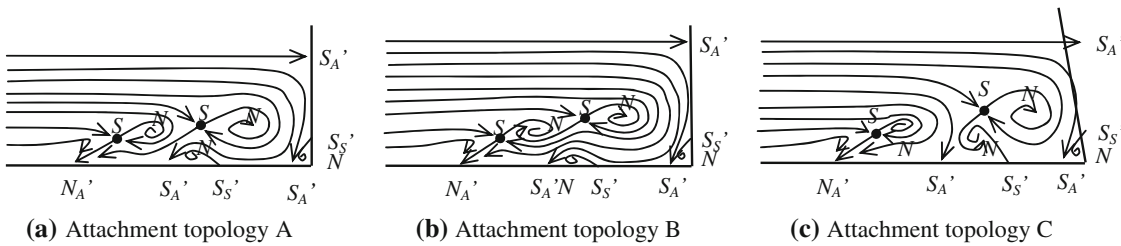
Fig. 17 Three topologies of attachment saddle point

(a) Attachment topology A   (b) Attachment topology B   (c) Attachment topology C
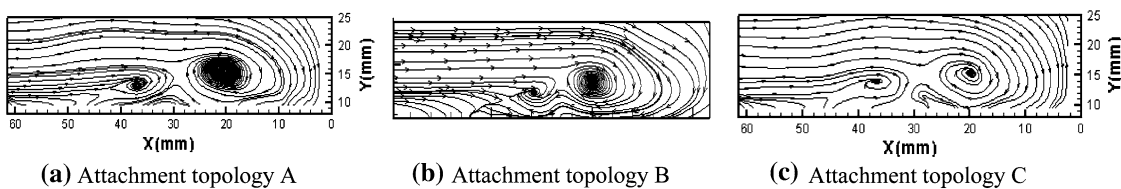
Fig. 18 PIV experimental confirmation of the three new topologies of attachment saddle point

topologies shown in Fig. 16 are named as stair-step (Norman 1972), jet maze (Norman, 1972) and alternative mode (Chen and Hung 1992), in which the streamline issued from the spatial saddle point attach to plate surface, engulf into upstream vortex or secondary vortex, respectively. Baker's (1979) smoke visualization in juncture flow revealed conventional separation stair-step mode of Fig 16a. Khan and Ahmed's (2005) fluorescent dye and hydrogen bubble visualization in juncture flow indicates three types of conventional separation topologies as shown in Fig 16a–c. The numerical simulations of Visbal (1991) and Chen and Hung (1992) revealed an attachment topology as shown in Fig. 17a. The PIV experiment results presented here reveal not only attachment topology of Fig. 17a but also the attachment topologies of Fig. 17b, c. The PIV experimental confirmation of the three attachment topologies is shown in Fig. 18. Attachment topologies in Fig. 17 and 18 are similar to those of conventional separated stair-step, jet maze and alternative mode in Fig. 16, apart from the outmost singular point on plate surface is an attachment saddle point. In addition to the common feature that outmost singular point on plate surface is an attachment saddle point, the streamline initiated from spatial saddle point may attach to plate surface, engulf into upstream vortex or secondary vortex as shown in Figs. 17 and 18. According to singular point topological rule given by Tobak and Peake (1979) and Hunt et al. (1978), the singular point index of local symmetry plane of juncture must satisfy following formula:

$$\left(\sum N + \frac{1}{2}\sum N'\right) - \left(\sum S + \frac{1}{2}\sum S'\right) = 0 \tag{1}$$

where $\sum N$ and $(\sum N')/2$ represents the summation of node index and half node index respectively, where as $\sum S$ and $(\sum S')/2$ represents the summation of saddle point index and half saddle point index, respectively. It is validated that not only conventional separation saddle point topologies in Fig. 16 but also attachment saddle point topologies in Fig. 17 satisfy above rule. Comparing conventional separation saddle point topology in Fig. 16b and attachment saddle point topology in Fig. 17b as example, in Fig. 16b $\sum N = 4$, $\sum N' = 0$, $\sum S = 1$, $\sum S' = 6$, and in Fig. 17b $\sum N = 4$, $\sum N' = 1$, $\sum S = 2$, $\sum S' = 5$; they all satisfy above formula (1).

The PIV results under discussion confirm the existence of attachment saddle point structure and do not deny the existence of conventional separation saddle point structure in juncture flow. As a matter of fact, two topologies can evolve from one to another under certain conditions, the influence parameters including Reynolds number, boundary layer characteristics, model section shape, and so on. A numerical simulation example of evolution between two topologies was shown in Figs. 12 and 13 which was taken from the simulation results of Wang et al. (2010). Detailed description of evolution of two topologies and parameters influence will be discussed in further experimental studies.

4 Conclusions

1. An experimental investigation of laminar juncture flows using PIV has confirmed the existence of attachment saddle point structures upstream of the cylinder juncture, in which the streamlines near surface do not rise up or separated from the surface but attach to the surface, the outmost vortex issues not from the plate surface but from a spatial saddle point.
2. Notably, the skin-friction-lines convergence corresponds to spatial attached flow but not separated flow as in case of conventional separation saddle point topology, alternatively the spatial attached flow correspond to convergent but not divergent skin-friction-lines, as happens in conventional attachment flows.
3. The attachment saddle point structure is a kind of separation in which vorticity separates from spatial layer of boundary layer but not from the plate surface.
4. The study reveals three types of attachment saddle point topologies, which are similar to those of stair-step mode, jet maze mode and alternative mode of conventional separation saddle point topologies, apart from the outmost singular point on plate surface is an attachment saddle point. These three topologies all satisfy the topological, singular point index rule of formula (1).
5. The PIV experimental confirmation about the existence of attachment saddle point topologies does not deny the existence of conventional separation saddle point topologies in juncture flow. Evolution of the two kind of topologies and parameters influence will be discussed in further studies.

References

Baker CJ (1979) The laminar horseshoe vortex. J Fluid Mech 95(2):347–367

Chen H (1995) Assessment of a Reynolds stress closure model for appendage–hull junction flows. J Fluid Eng l l7:557–563

Chen CL, Hung CM (1992) Numerical study of juncture flows. AIAA J 30(7):1800–1807

Coon MD, Tobak M (1995) Experimental study of saddle point of attachment in laminar juncture flow. AIAA J 33(22):88–92 (AIAA 95-0785)

Hung CM, Sung CH, Chen CL (1992) Computation of saddle point of attachment. AIAA J 30(6):1561–1569

Hunt JCR, Abell CJ, Peterka JA, Woo H (1978) Kinematical studies of the flows around free or surface-mounted obstacles; applying topology to flow visualization. J Fluid Mech 86(1):179–200

Khan MJ, Ahmed A (2005) Topological model of flow regimes in the plane of symmetry of a surface-mounted obstacle. Phys Fluids 17:045101 (1–8)

Lighthill MJ (1963) Laminar boundary layers. In: Rosenhead L (ed) Oxford University Press, USA, pp 5–88

Maskell EC (1955) Flow separation in three dimension: RAE aero report, pp 2655–2673

Norman RS (1972) On obstacle generated secondary flows in laminar boundary layers and transition to turbulence: Ph.D dissertation. Illinois Institute of Technology, Chicago

Perry AE, Fairlie BW (1974) Critical points in flow patterns. Adv Geophys 18B:299–315

Puhak RL, Degani AT, Walker JDA (1995) Unsteady separation and heat transfer upstream of obstacles. J Fluid Mech 305:1–27

Rizetta DP (1994) Numerical simulation of turbulent cylinder juncture flow fields. AIAA J 32(6):1113–1119

Seal CV, Smith CR, Akin O, Rockwell D (1995) Quantitative characteristics of a laminar, unsteady necklace vortex system at a rectangular block-flat juncture. J Fluid Mech 286:117–135

Seal CV, Smith CR, Rockwell D (1997) Dynamics of the vorticity distribution in endwall junctions. AIAA J 35(6):1041–1047

Tobak M, Peake DJ (1979) Topology of two-dimensional and three-dimensional separated flows. AIAA Paper 79:1480

Visbal MR (1991) Structure of laminar juncture flows. AIAA J 29(8):1273–1282

Wang KC (1972) Separation patterns of boundary layer over an inclined body of revolution. AIAA 10(8):1044–1050

Wang KC (1976) Separation of three-dimensional flow. MML 76:54

Wang X, Zhang H, Wang H, Fu L (2010) New 3-D separation structure in juncture flows. J Beijing Univ Aeronaut Astronaut 36(12):1461–1466 (in Chinese)

Zhang HX (2005) Structural analysis of separated flows and vortex motion. National Defense Industry Press, Beijing (in Chinese)